

Supporting Information

Slow Magnetic Relaxation in $\text{Co}^{\text{II}}\text{--Ln}^{\text{III}}$ Heterodinuclear Complexes Achieved through Functionalized Nitronyl Nitroxide Biradical

Lu Xi, Juan Sun, Kang Wang, Jiao Lu, Pei Jing, and Licun Li*

Department of Chemistry, Key Laboratory of Advanced Energy Materials Chemistry,
College of Chemistry, Nankai University, Tianjin 300071, China

*E-mail: llicun@nankai.edu.cn.

Table S1. Crystallographic data for **1–5**.

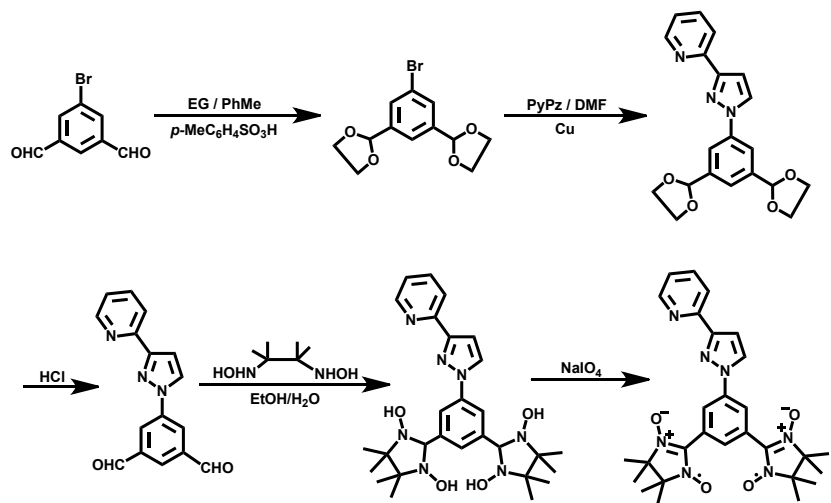
Complex	1 YCo	2 GdCo	3 TbCo	4 DyCo	5 HoCo
Formula	$C_{54}H_{40}Cl_2CoF_{30}LnN_7O_{14}$				
$M(g \cdot mol^{-1})$	1799.67	1868.01	1869.68	1873.26	1875.69
$T(K)$	113(2)	150(2)	113(2)	113(2)	150(2)
Crystal system	triclinic	triclinic	Triclinic	triclinic	triclinic
Space group	$P\bar{1}$	$P\bar{1}$	$P\bar{1}$	$P\bar{1}$	$P\bar{1}$
$a(\text{\AA})$	12.187(2)	12.2121(5)	12.211(2)	12.180(2)	12.1364(3)
$b(\text{\AA})$	13.349(3)	13.2856(6)	13.355(3)	13.325(3)	13.2997(3)
$c(\text{\AA})$	23.253(5)	23.3097(12)	23.318(5)	23.270(5)	23.2102(6)
$\alpha(\text{deg})$	91.97(3)	92.167(4)	92.09(3)	92.00(3)	91.971(2)
$\beta(\text{deg})$	103.85(3)	103.998(4)	104.23(3)	104.14(3)	104.109(2)
$\gamma(\text{deg})$	105.47(3)	105.463(4)	105.23(3)	105.32(3)	105.537(2)
$V(\text{\AA}^3)$	3520.3(14)	3515.5(3)	3535.7(14)	3512.1(14)	3480.60(15)
Z	2	2	2	2	2
$D_{\text{calcd}}(g \cdot cm^{-3})$	1.698	1.765	1.756	1.771	1.790
$M(mm^{-1})$	1.275	1.391	1.445	1.512	1.589
$\theta(\text{deg})$	1.592–25.010	3.000–25.010	1.590–25.010	1.594–25.008	2.931–25.010
$F(000)$	1790	1840	1842	1844	1846
Reflns	34207	28714	31063	33402	28291
Unique	12403/0.0624	12385/0.0360	12419/0.0559	12378/0.0959	12266/0.0468
GOF(F^2)	1.001	1.004	1.010	1.007	1.010
$R_1/wR_2(I > 2\sigma(I))$	0.0685/0.170	0.0528/0.151	0.0752/0.181	0.0614/0.170	0.0406/0.091
$R_1/wR_2(\text{all data})$	0.0961/0.192	0.0651/0.161	0.0881/0.203	0.0776/0.195	0.0589/0.100

Table S2. Selected bond lengths [Å] and bond angles [°] for **1–2**.

	1 YCo		2 GdCo
Y(1)–O(2)	2.389(4)	Gd(1)–O(2)	2.426(4)
Y(1)–O(3)	2.285(4)	Gd(1)–O(3)	2.326(4)
Y(1)–O(4)	2.381(4)	Gd(1)–O(4)	2.424(4)
Y(1)–O(5)	2.362(4)	Gd(1)–O(5)	2.398(4)
Y(1)–O(6)	2.293(4)	Gd(1)–O(6)	2.332(4)
Y(1)–O(7)	2.325(4)	Gd(1)–O(7)	2.362(4)
Y(1)–O(8)	2.351(4)	Gd(1)–O(8)	2.395(4)
Y(1)–O(9)	2.327(3)	Gd(1)–O(9)	2.366(4)
Co(1)–O(11)	2.050(4)	Co(1)–O(11)	2.054(4)
Co(1)–O(12)	2.063(4)	Co(1)–O(12)	2.062(4)
Co(1)–O(13)	2.070(4)	Co(1)–O(13)	2.074(4)
Co(1)–O(14)	2.065(4)	Co(1)–O(14)	2.067(4)
Co(1)–N(6)	2.133(4)	Co(1)–N(6)	2.144(4)
Co(1)–N(7)	2.134(4)	Co(1)–N(7)	2.128(5)
N(6)–N(5)	1.354(5)	N(6)–N(5)	1.350(6)
O(1)–N(1)	1.274(5)	O(1)–N(1)	1.270(6)
O(2)–N(2)	1.309(5)	O(2)–N(2)	1.296(6)
O(9)–N(3)	1.304(5)	O(9)–N(3)	1.301(6)
O(10)–N(4)	1.263(5)	O(10)–N(4)	1.248(7)
O(9)–Y(1)–O(2)	83.73(13)	O(9)–Gd(1)–O(2)	83.92(13)
O(3)–Y(1)–O(4)	72.33(13)	O(3)–Gd(1)–O(4)	71.47(15)
O(6)–Y(1)–O(5)	71.47(13)	O(6)–Gd(1)–O(5)	70.61(15)
O(7)–Y(1)–O(8)	73.01(13)	O(7)–Gd(1)–O(8)	72.01(14)
N(6)–Co(1)–N(7)	76.87(16)	N(6)–Co(1)–N(7)	76.61(17)
O(11)–Co(1)–O(12)	88.10(15)	O(11)–Co(1)–O(12)	88.02(16)
O(14)–Co(1)–O(13)	85.90(15)	O(14)–Co(1)–O(13)	85.60(18)

Table S3. Selected bond lengths [Å] and bond angles [°] for **3–5**.

3 TbCo		4 DyCo		5 HoCo	
Tb(1)–O(2)	2.429(6)	Dy(1)–O(2)	2.416(5)	Ho(1)–O(2)	2.387(3)
Tb(1)–O(3)	2.328(7)	Dy(1)–O(3)	2.306(5)	Ho(1)–O(3)	2.295(3)
Tb(1)–O(4)	2.408(7)	Dy(1)–O(4)	2.402(5)	Ho(1)–O(4)	2.385(3)
Tb(1)–O(5)	2.393(7)	Dy(1)–O(5)	2.379(5)	Ho(1)–O(5)	2.359(3)
Tb(1)–O(6)	2.334(7)	Dy(1)–O(6)	2.318(5)	Ho(1)–O(6)	2.297(3)
Tb(1)–O(7)	2.357(6)	Dy(1)–O(7)	2.337(5)	Ho(1)–O(7)	2.323(3)
Tb(1)–O(8)	2.385(7)	Dy(1)–O(8)	2.364(6)	Ho(1)–O(8)	2.348(3)
Tb(1)–O(9)	2.365(6)	Dy(1)–O(9)	2.344(5)	Ho(1)–O(9)	2.327(3)
Co(1)–O(11)	2.061(6)	Co(1)–O(11)	2.050(5)	Co(1)–O(11)	2.059(3)
Co(1)–O(12)	2.068(7)	Co(1)–O(12)	2.070(5)	Co(1)–O(12)	2.064(3)
Co(1)–O(13)	2.077(7)	Co(1)–O(13)	2.072(5)	Co(1)–O(13)	2.074(3)
Co(1)–O(14)	2.073(7)	Co(1)–O(14)	2.078(5)	Co(1)–O(14)	2.064(3)
Co(1)–N(6)	2.150(7)	Co(1)–N(6)	2.147(6)	Co(1)–N(6)	2.139(3)
Co(1)–N(7)	2.134(8)	Co(1)–N(7)	2.125(6)	Co(1)–N(7)	2.123(4)
N(6)–N(5)	1.355(10)	N(6)–N(5)	1.345(8)	N(6)–N(5)	1.352(4)
O(1)–N(1)	1.277(10)	O(1)–N(1)	1.270(8)	O(1)–N(1)	1.273(5)
O(2)–N(2)	1.299(9)	O(2)–N(2)	1.290(7)	O(2)–N(2)	1.295(4)
O(9)–N(3)	1.319(10)	O(9)–N(3)	1.319(8)	O(9)–N(3)	1.304(4)
O(10)–N(4)	1.262(11)	O(10)–N(4)	1.266(8)	O(10)–N(4)	1.261(5)
O(9)–Tb(1)–O(2)	83.5(2)	O(9)–Dy(1)–O(2)	83.47(17)	O(9)–Ho(1)–O(2)	83.82(9)
O(3)–Tb(1)–O(4)	71.6(2)	O(3)–Dy(1)–O(4)	71.75(19)	O(3)–Ho(1)–O(4)	72.33(10)
O(6)–Tb(1)–O(5)	71.3(2)	O(6)–Dy(1)–O(5)	71.22(17)	O(6)–Ho(1)–O(5)	71.73(11)
O(7)–Tb(1)–O(8)	72.4(2)	O(7)–Dy(1)–O(8)	72.76(18)	O(7)–Ho(1)–O(8)	73.15(10)
N(6)–Co(1)–N(7)	76.8(3)	N(6)–Co(1)–N(7)	76.6(2)	N(6)–Co(1)–N(7)	76.77(13)
O(11)–Co(1)–O(12)	87.9(3)	O(11)–Co(1)–O(12)	88.19(19)	O(11)–Co(1)–O(12)	88.11(11)
O(14)–Co(1)–O(13)	85.9(3)	O(14)–Co(1)–O(13)	85.9(2)	O(14)–Co(1)–O(13)	85.73(12)



Scheme S1. The synthesis of NITPh-PyPzbis biradical ligand (EG: ethylene glycol, PyPz: 2-(1H-pyrazol-3-yl)pyridine).

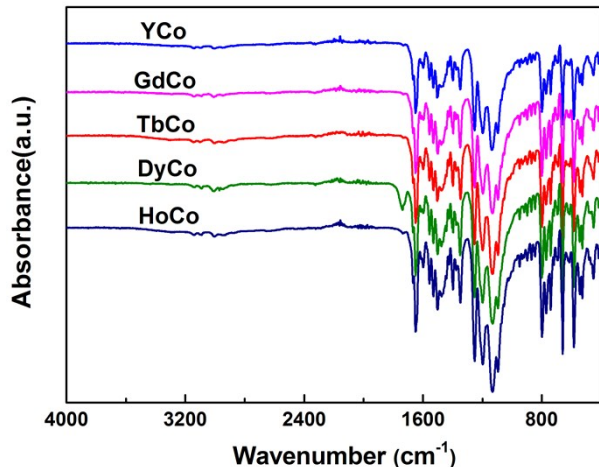


Figure S1. The IR spectra for compounds **1–5**.

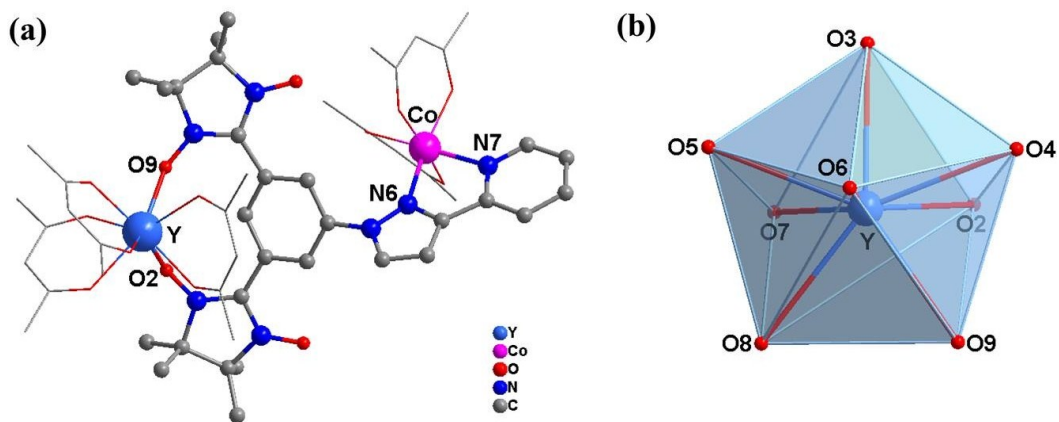


Figure S2. (a) The dinuclear structure of **1** (H, F, and CH_2Cl_2 are omitted). Color code: light blue-Y, pink-Co, gray-C, red-O, blue-N. (b) Coordination polyhedron of lanthanide Y in **1**.

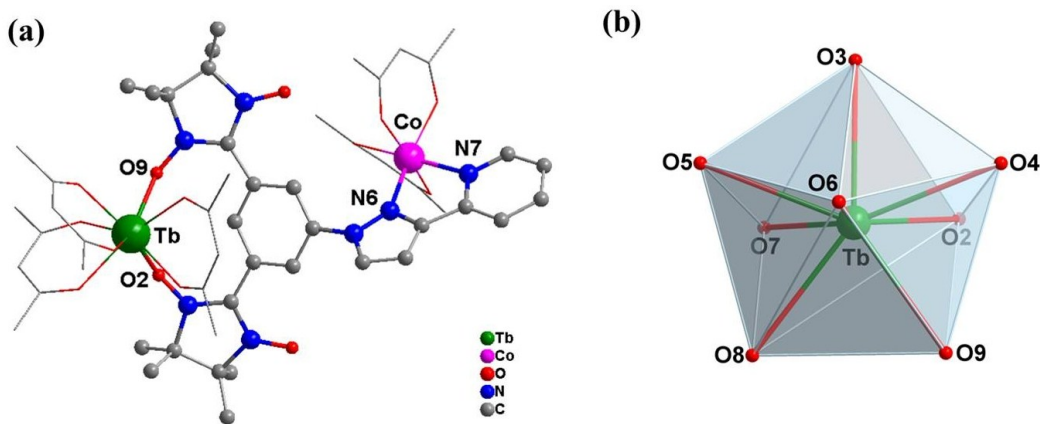


Figure S3. (a) The dinuclear structure of **3** (H, F, and CH_2Cl_2 are omitted). Color code: green-Tb, pink-Co, gray-C, red-O, blue-N. (b) Coordination polyhedron of lanthanide Tb in **3**.

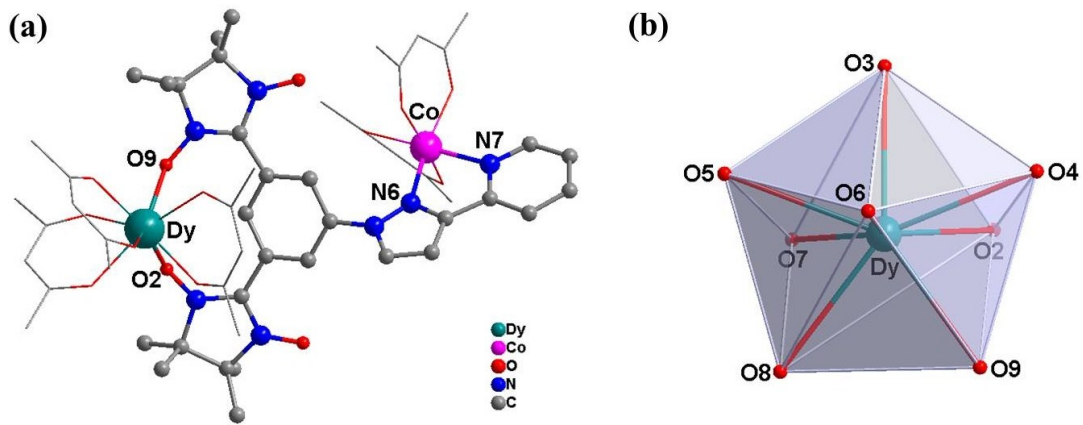


Figure S4. (a) The dinuclear structure of **4** (H, F, and CH_2Cl_2 are omitted). Color code: teal-Dy, pink-Co, gray-C, red-O, blue-N. (b) Coordination polyhedron of lanthanide Dy in **4**.

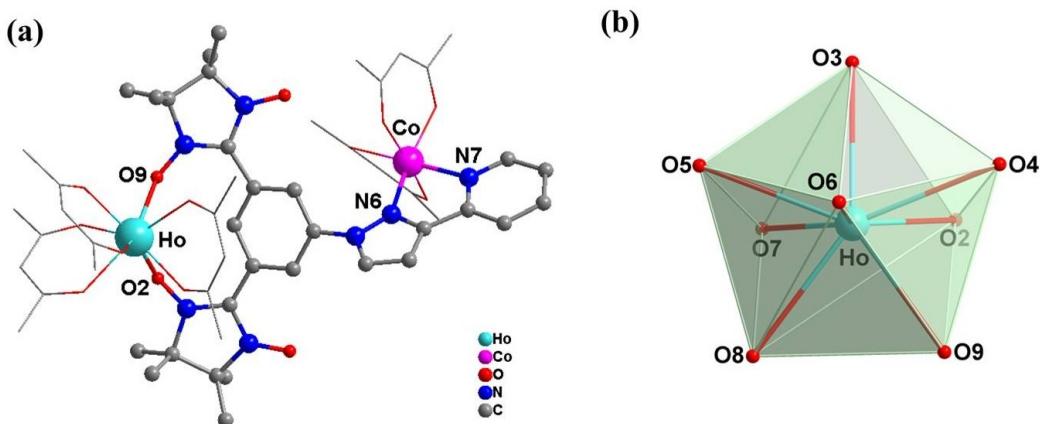


Figure S5. (a) The dinuclear structure of **5** (H, F, and CH_2Cl_2 are omitted). Color code: aqua-Ho, pink-Co, gray-C, red-O, blue-N. (b) Coordination polyhedron of lanthanide Ho in **5**.

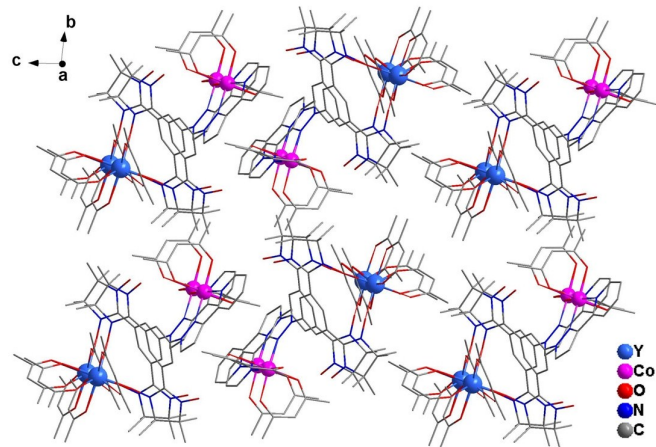


Figure S6. Packing diagram of **1** (H, F, and CH₂Cl₂ are omitted).

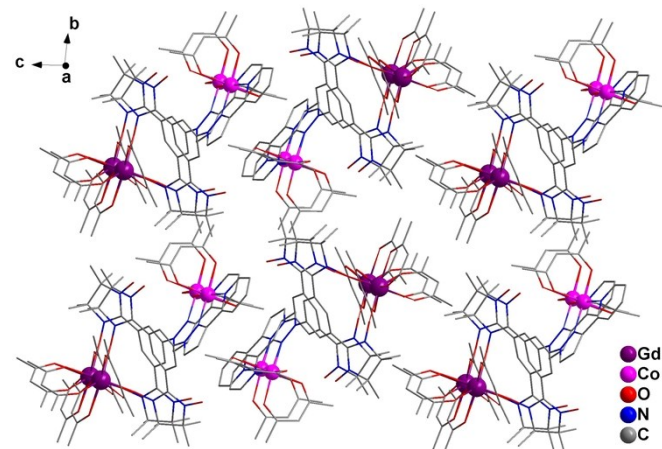


Figure S7. Packing diagram of **2** (H, F, and CH₂Cl₂ are omitted).

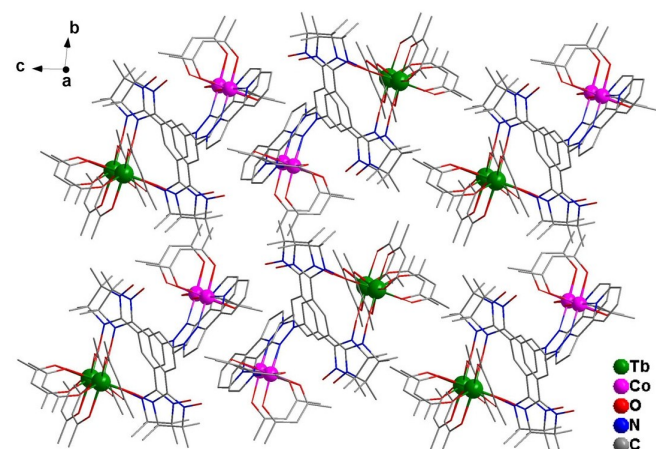


Figure S8. Packing diagram of **3** (H, F, and CH₂Cl₂ are omitted).

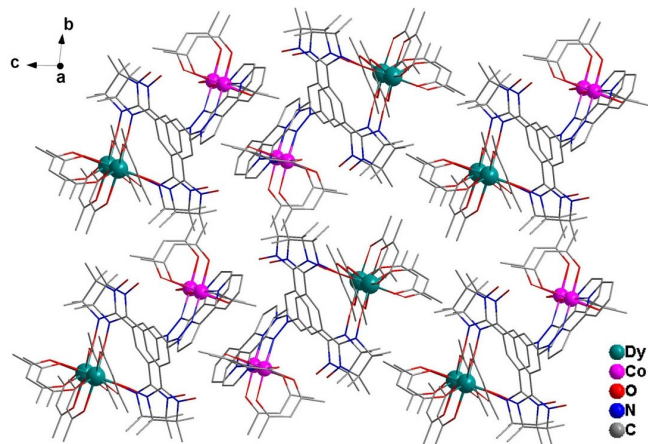


Figure S9. Packing diagram of **4** (H, F, and CH_2Cl_2 are omitted).

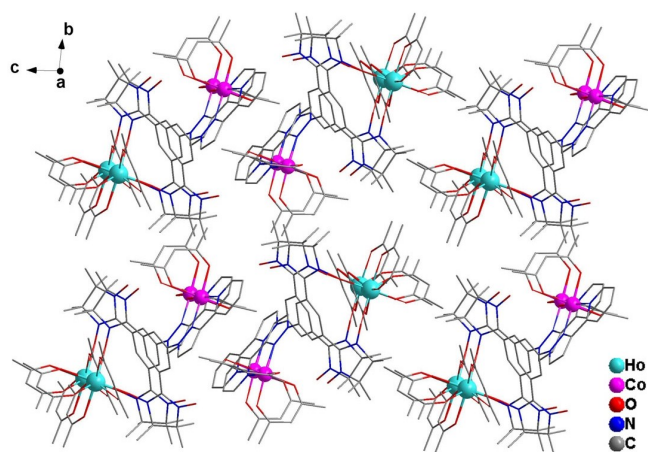


Figure S10. Packing diagram of **5** (H, F, and CH_2Cl_2 are omitted).

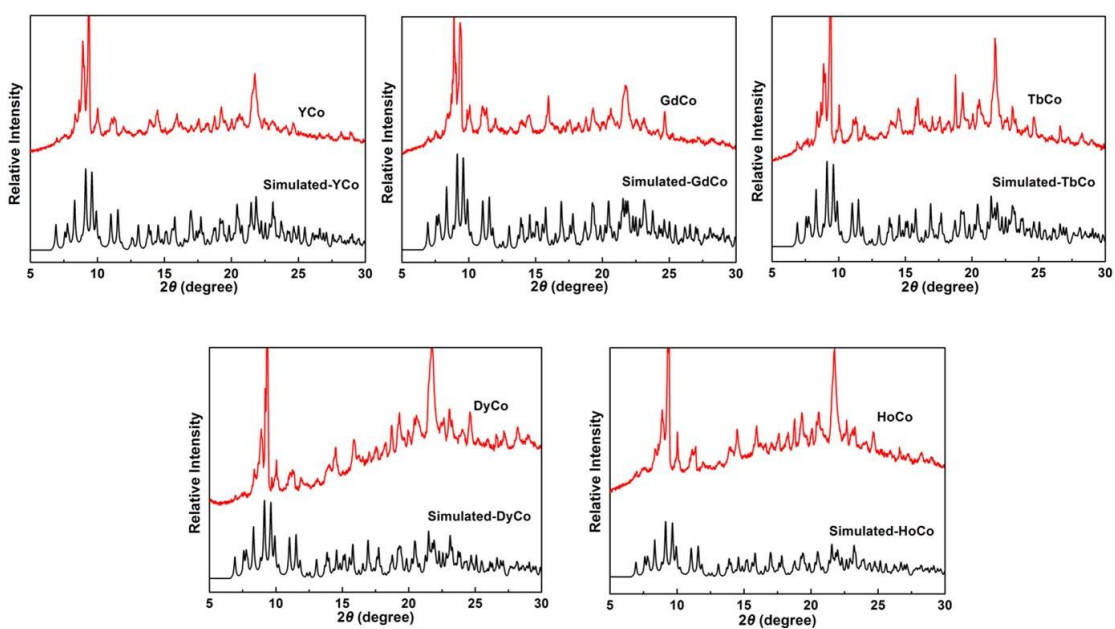


Figure S11. The Powder X-ray diffraction (PXRD) patterns for complexes **1–5** at room temperature.

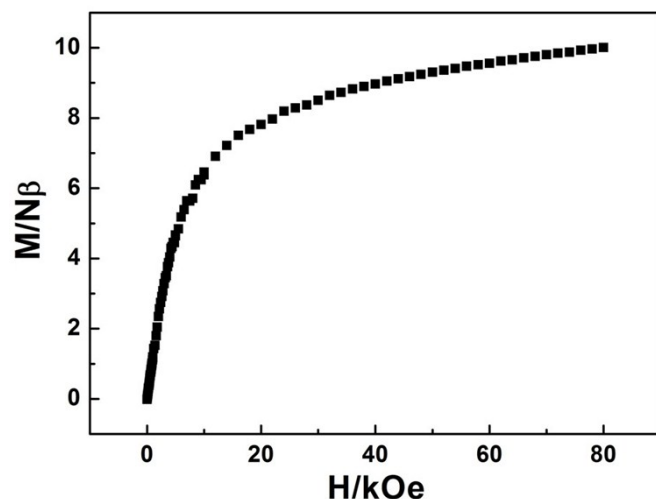


Figure S12. M vs H plot for **3** at 2 K.

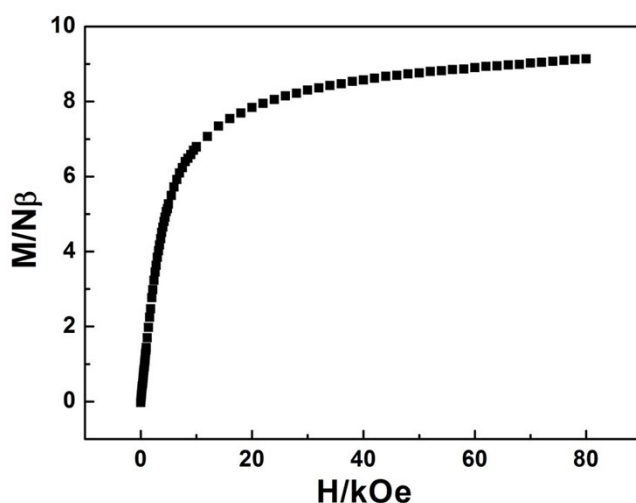


Figure S13. M vs H plot for **4** at 2 K.

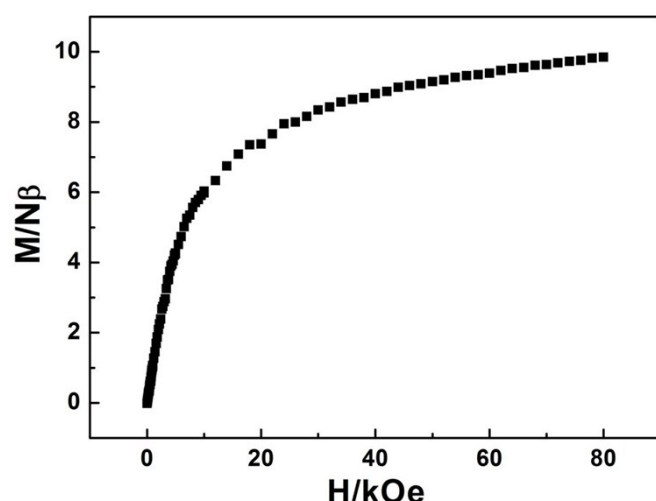


Figure S14. M vs H plot for **5** at 2 K.

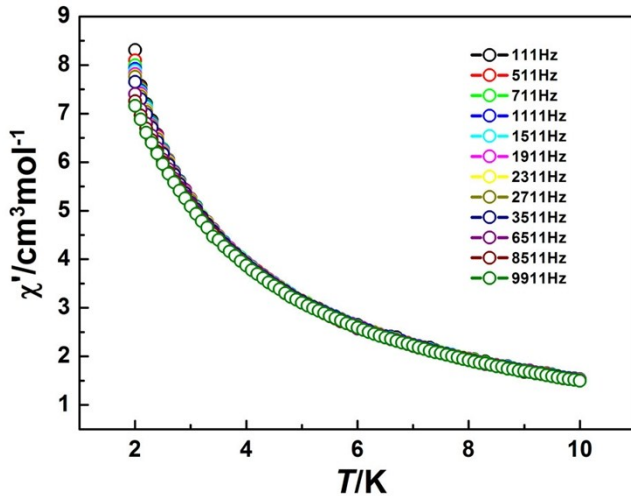


Figure S15. Temperature dependence of χ' for **4** in zero dc field.

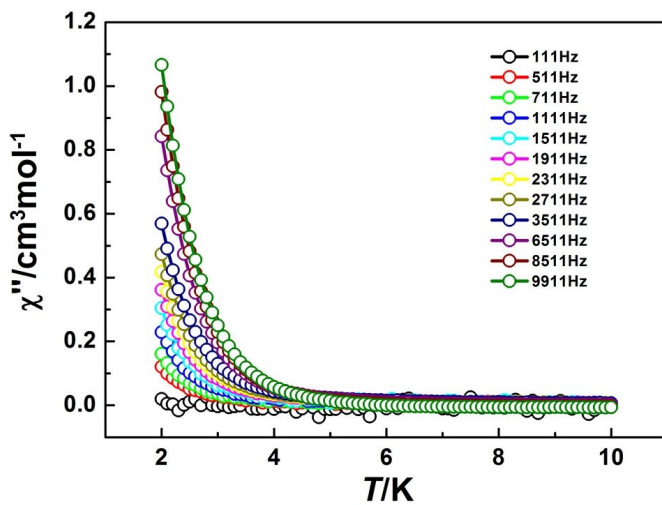


Figure S16. Temperature dependence of χ'' for **4** in zero dc field.

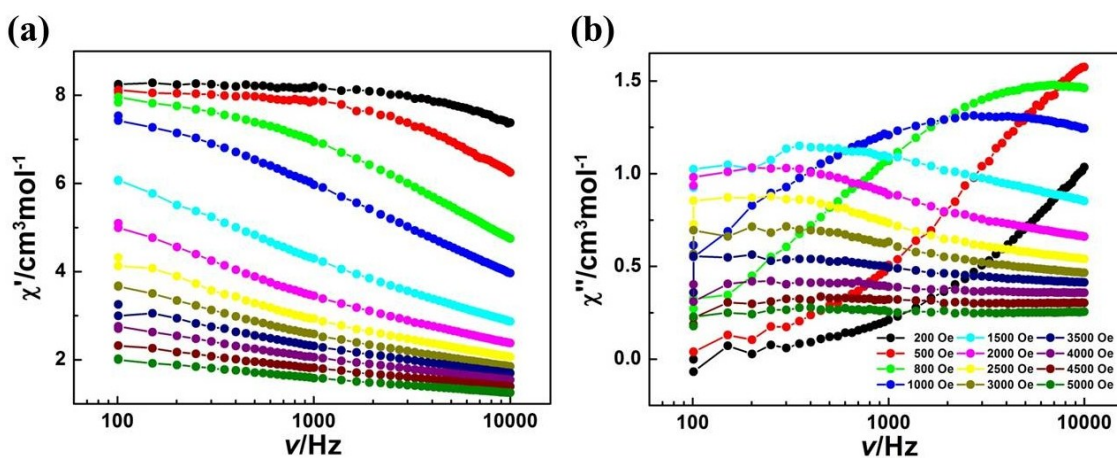


Figure S17. Frequency dependencies of χ' (a) and χ'' (b) for **4** in the dc fields of 200–5000 Oe.

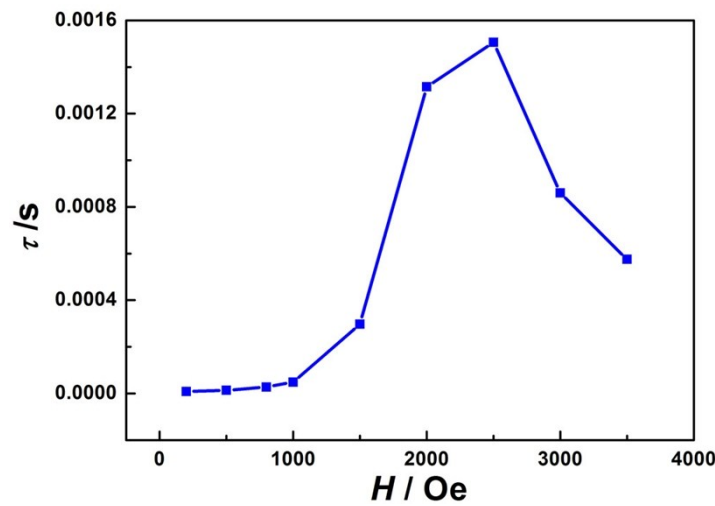


Figure S18. The τ vs H plot for **4** at 2 K under applied dc fields.

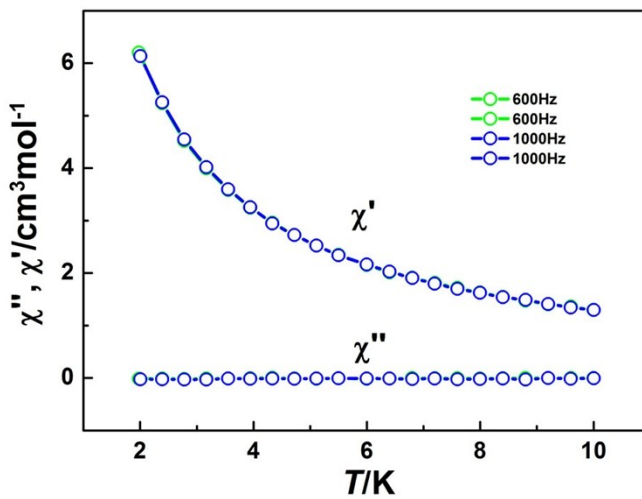


Figure S19. Temperature dependencies of χ' and χ'' for **2** in zero dc field.

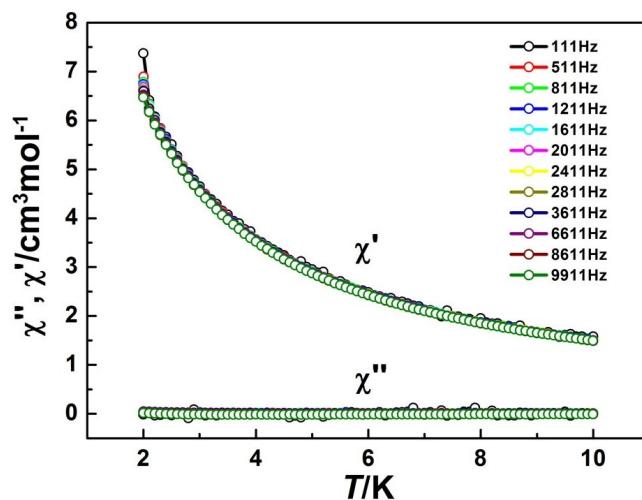


Figure S20. Temperature dependencies of χ' and χ'' for **3** in zero dc field.

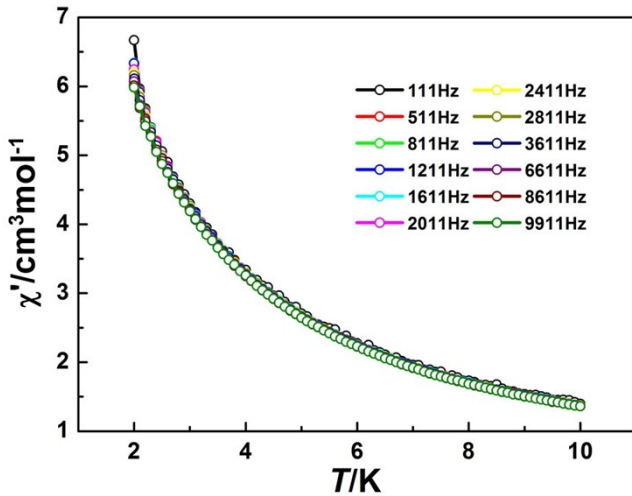


Figure S21. Temperature dependence of χ' for **5** in zero dc field.

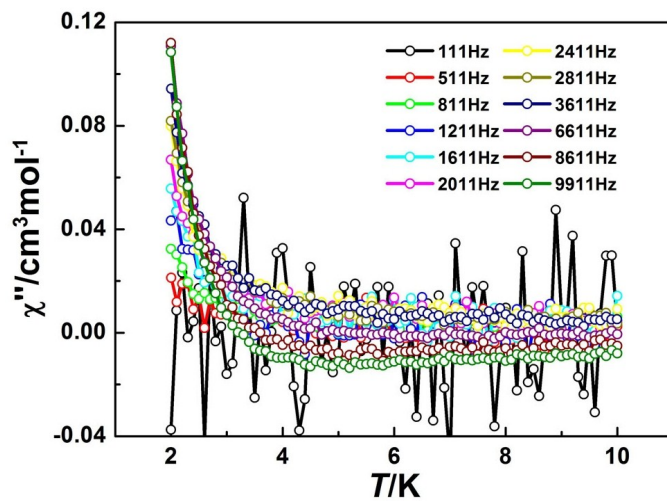


Figure S22. Temperature dependence of χ'' for **5** in zero dc field.

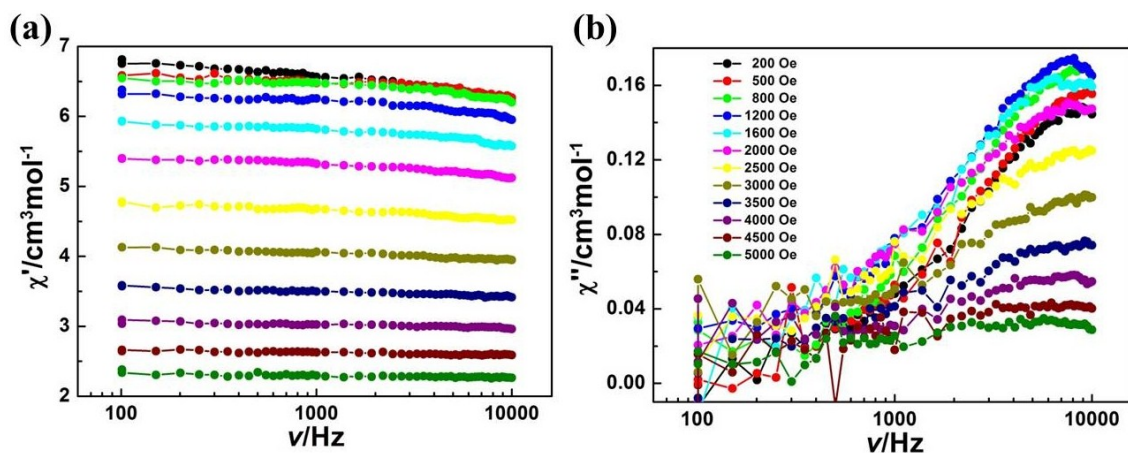


Figure S23. Frequency dependencies of χ' (a) and χ'' (b) for **5** in the dc fields of 200–5000 Oe.